Observation of phonon peaks and electron-phonon bound states in graphene

Yu Zhang,[1] Qian Yang,[1] Ya-Ning Ren,[1] and Lin He[1,2,*]

[1]*Center for Advanced Quantum Studies, Department of Physics, Beijing Normal University, Beijing 100875, People's Republic of China*

[2]*State Key Laboratory of Functional Materials for Informatics, Shanghai Institute of Microsystem and Information Technology, Chinese Academy of Sciences, 865 Changning Road, Shanghai 200050, People's Republic of China*

(Received 8 April 2019; revised manuscript received 11 August 2019; published 28 August 2019)

Theoretically, coupling of phonons with quasiparticles in the Landau levels (LLs) of graphene was predicted to generate a new sequence of discrete states in the density of states, i.e., phonon peaks. However, it was believed that these phonon peaks are extremely weak due to weak electron-phonon coupling in graphene. Here, we report the experimental observation of giant phonon peaks in a graphene monolayer induced by enhanced electron-phonon coupling. We demonstrate that emission or absorption of phonons of quasiparticles in the LLs of graphene generates the phonon peaks, which even exhibits fine structures corresponding to bound states of an electron and of a phonon. We also show that it is possible to tune the relative strength of the phonon peaks at nanoscale by controlling interactions between graphene and the supporting substrate. The local strain in graphene may play a vital role in enhancing the electron-phonon coupling, which results in the observed giant phonon peaks. Our experiment indicates that it is possible to explore interesting emergent phenomena, such as superconductivity, induced by electron-phonon coupling in graphene.

DOI: 10.1103/PhysRevB.100.075435

I. INTRODUCTION

Electronic properties of materials can be strongly modified by phonons through electron-phonon coupling [1]. A well-known phenomenon induced by electron-phonon coupling is the emergence of superconductivity in Bardeen-Cooper-Schrieffer (BCS) superconductors [2,3]. However, the strength of electron-phonon coupling in intrinsic graphene is usually negligible due to the extremely weak electron-phonon pairing potential and a vanishing density of states (DOS) near the Dirac point [4–18]. Therefore, it should be quite difficult to observe interesting emergent phenomena via DOS in graphene induced by the electron-phonon coupling. In this paper, we report the experimental observation of a sequence of phonon peaks in graphene monolayer. Our work demonstrates that emission or absorption of the K and K' out-of-plane phonon of electrons in the Landau levels (LLs) of graphene results in the emergence of giant phonon peaks which exhibit magnetic-field-independent fine structures due to the electron-phonon interaction. We also demonstrate the ability to turn the relative strength of these phonon peaks at nanoscale. Our experiment indicates that the local strain in graphene may play a vital role in enhancing the electron-phonon coupling. Such a result suggests that it is possible to realize a BCS superconducting state in deformed graphene [19,20].

Among all the phonons in graphene, the K and K' out-of-plane phonon really stands out: it introduces a new inelastic tunneling channel in the perpendicular direction of graphene and generates a gaplike feature (with a "gap" of about 130 meV) exactly at the Fermi level (E_F). Such a characteristic feature is detectable in the absence of magnetic field and has been extensively observed in the studies of graphene by using both scanning tunneling spectroscopy (STS) [21–29] and angle-resolved photoemission spectroscopy (ARPES) [30–32]. In our experiment, the phonon peaks are detected in high magnetic fields via STS measurements. In the tunneling spectra, the intensity of the observed phonon peaks of the K and K' out-of-plane phonon is about 50 times larger than that of the LLs because the phonon opens an inelastic tunneling channel.

II. EXPERIMENTAL OBSERVATION OF THE PHONON PEAKS

In our experiment, the graphene monolayer is directly synthesized on Cu foils via a traditional low-pressure chemical vapor deposition (LPCVD) method, and then the transfer-assisted method is adopted to transfer the graphene sheet onto 300-nm SiO_2/Si wafers [6,33,34]. We transfer three layers of graphene on SiO_2/Si wafers, and the underlying two graphene sheets are used to reduce any possible interactions between the topmost graphene sheet and the substrate (see Supplemental Material (SM) Figs. S1 and S2 [35]). Our experiment indicates that this layer-by-layer transfer process can effectively reduce the interlayer coupling, leaving the topmost graphene sheet behaves as a pristine graphene monolayer. Figure 1(a) shows a representative scanning tunneling microscopy (STM) image of a decoupled graphene region. Due to the roughness of the underlying SiO_2/Si wafers, there exist surface corrugations with a vertical dimension of ~80 pm, leaving some nanoscale graphene regions suspended. Figure 1(b) shows a typical dI/dV spectrum recorded on a suspended graphene region, exhibiting a gaplike feature of approximately 130 meV pinned to E_F. Such a gaplike feature, which has been demonstrated

*Corresponding author: helin@bnu.edu.cn

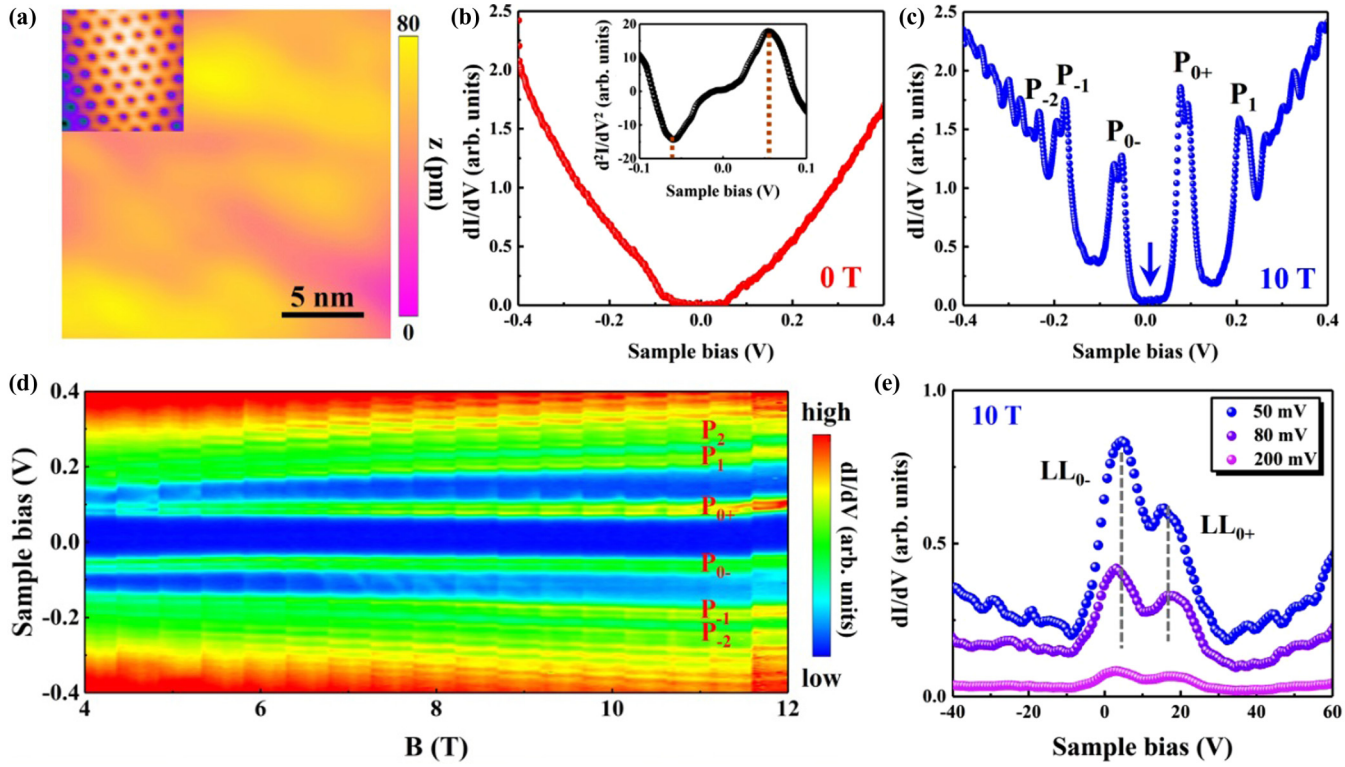

FIG. 1. The inelastic tunneling spectra of suspended graphene monolayer under different magnetic fields. (a) A $20 \times 20\,\mathrm{nm}^2$ STM image of a suspended graphene region ($V_b = 0.3\,\mathrm{mV}$, $I = 0.1\,\mathrm{nA}$). Inset: Zoom-in atomic-resolution STM topography. (b) The average of a series of dI/dV spectra acquired in panel (a) at $B = 0\,\mathrm{T}$. The central gaplike feature is attributed to the K and K' out-of-plane phonons with energy $\hbar\omega_{ph} \approx 65$ meV in suspended graphene monolayer. Inset: d^2I/dV^2 spectra acquired in panel (a) at $B = 0\,\mathrm{T}$. (c) The average of a series of dI/dV spectra acquired in panel (a) at $B = 10\,\mathrm{T}$. P_N labels the phonon peaks, which are induced by the intrinsic LLs coupling to the K and K' out-of-plane phonons. (d) The evolution of a series of inelastic electron tunneling spectra as a function of magnetic fields B from 4 to 12 T as a variation of 0.5 T. Each panel of every B consists of 30 dI/dV spectra acquired at different spatial points along a line of 20 nm. (e) Enlarged dI/dV spectra within the gap marked by a blue arrow in panel (c) measured with the different V_b and in the magnetic field of $B = 10\,\mathrm{T}$ ($I = 0.4\,\mathrm{nA}$). The LL_0 can be clearly seen inside the gap under low V_b.

explicitly in previous STM [21–29], inelastic x-ray scattering [36], and ARPES experiments [30–32], is attributed to the phonon-mediated inelastic tunneling. We can directly deduce the energy of the K and K' out-of-plane phonons, $\sim$65 meV, from the corresponding d^2I/dV^2 spectrum, as shown in inset of Fig. 1(b).

Figure 1(c) shows a representative dI/dV spectrum recorded on the suspended graphene region in a magnetic field of $B = 10\,\mathrm{T}$. Strikingly, the spectrum exhibits a sequence of pronounced peaks which are almost symmetric about E_F and show different features from that of the LLs in graphene monolayer. To explore the exact nature of these peaks, we carry out STS measurements under different magnetic fields. Figure 1(d) shows evolution of the dI/dV spectra as a function of magnetic fields B from 4 to 12 T as a variation of 0.5 T. Each panel of every magnetic field consists of 30 dI/dV spectra acquired at different spatial points along a line of 20 nm. The spectra recorded at different positions are reproducible, indicating that the peaks in the spectra are only controlled by the magnetic fields. A notable feature is that there are two magnetic-field-independent peaks on both sides of the E_F (P_{0+} and P_{0-}) with the energy separation $\sim$130 meV, which is the same as the gaplike feature generated by the K and K' out-of-plane phonons in zero magnetic field. Simultaneously, there are several peaks, marked with P_N ($N \neq 0$), depending on the square root of both level index N and magnetic field B (SM Fig. S3 [35]). Obviously, the behavior of the peaks P_N is similar to that of the LL_N for massless Dirac fermions in graphene monolayer with only a shift of $\sim$65 meV in energy [37,38]. A close examination of the low-bias spectra also reveals the existence of the zero LL (LL_0) around the Fermi level, as shown in Fig. 1(e) (SM Fig. S4 [35]). All the experimental results indicate that the K and K' out-of-plane phonons play a vital role in the emergence of the new discrete states in graphene monolayer in magnetic fields.

In the absence of magnetic field, the K and K' out-of-plane phonons mix the nearly free-electron bands at Γ and the linear π bands of graphene and create new inelastic tunneling channels in the perpendicular direction of graphene [21,39]. Since Pauli's exclusion principle blocks electron tunneling into occupied states, there exists a threshold energy $\hbar\omega_{ph}$, determined by the vibrational frequency ω_{ph}, below which the inelastic scattering process cannot happen (in our experiment, $\hbar\omega_{ph} \sim 65$ meV is the energy of the K and K' out-of-plane phonons). Therefore, we can detect a gaplike feature with energy $\sim 2\hbar\omega_{ph}$ in the tunneling spectra of graphene monolayer, as schematically shown in Fig. 2(a) and experimentally observed in Fig. 1(b). By applying a perpendicular magnetic

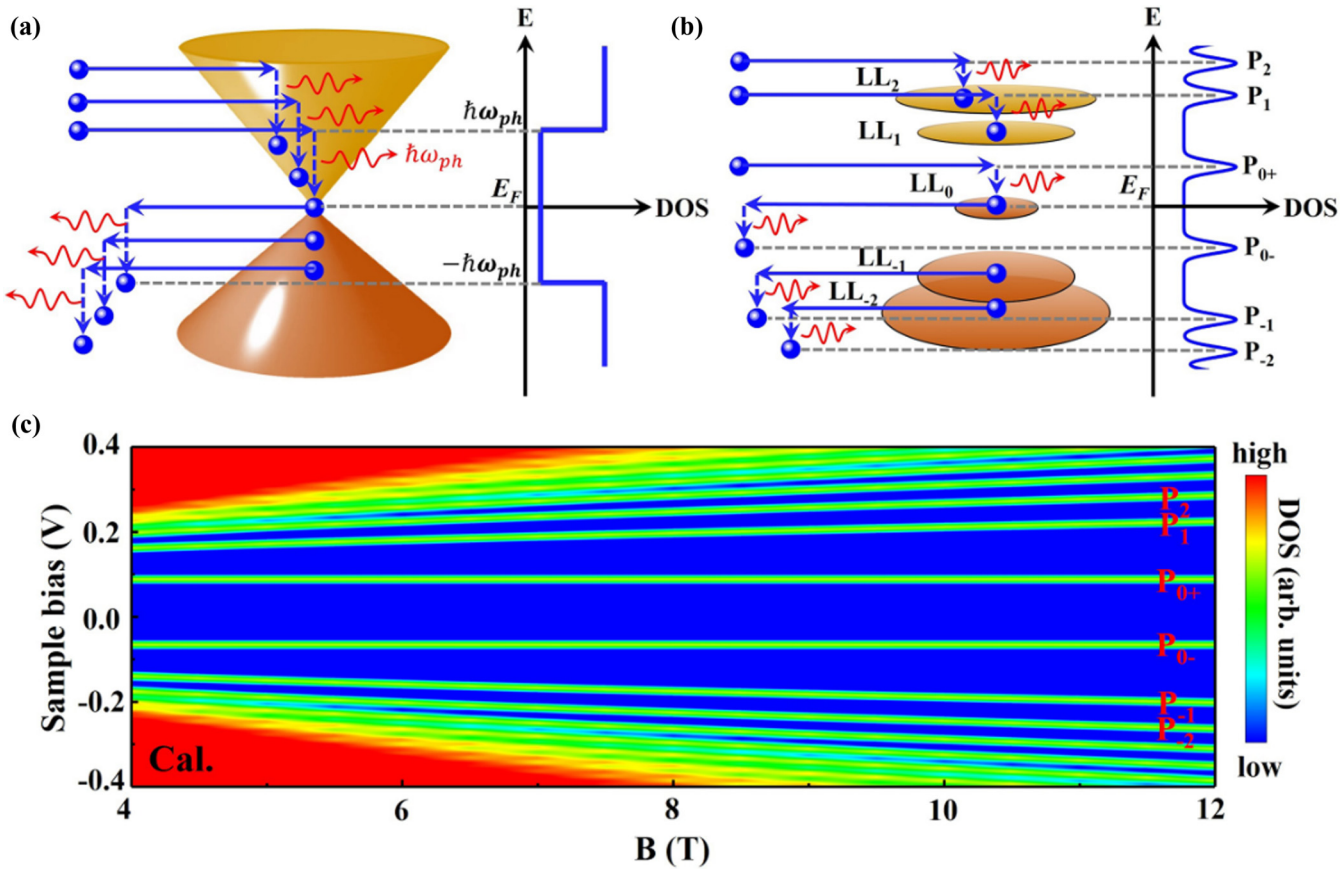

FIG. 2. Schematic images of the inelastic electron tunneling spectra in graphene monolayer under different magnetic fields. (a) Schematic of the inelastic electron tunneling due to excitation of phonons with energy $\hbar\omega_{ph}$ at $B = 0$ T. The low-energy electronic structures for graphene show the two Dirac cones that meet at the Dirac point (E_D), where the density of carriers vanishes. The tunnel current is abruptly enhanced if the energy is high enough to excite a phonon with threshold energy of $\hbar\omega_{ph}$, thus opening a new inelastic tunneling channel at energies of $\pm\hbar\omega_{ph}$ and causing steps in DOS symmetric to E_F. (b) Schematic of the inelastic electron tunneling due to excitation of phonons with energy $\hbar\omega_{ph}$ at $B > 0$ T. The intrinsic LLs are shown as the numbered disks. (c) Calculations of the B-dependent DOS of the suspended graphene monolayer by considering the coupling of electron LLs and the K and K' out-of-plane phonons.

field, the massless Dirac fermions in the graphene monolayer are condensed into discrete LLs. Then a new set of peaks at energies $E_N + \hbar\omega_{ph}$ for $E_N > E_F$ and $E_N - \hbar\omega_{ph}$ for $E_N < E_F$ is expected to be introduced, corresponding to the emission or absorption of phonons in the tunneling process, as schematically shown in Fig. 2(b). Therefore, the observed peaks in Figs. 1(c) and 1(d) should be attributed to the phonon peaks of the K and K' out-of-plane phonons in graphene. Previously, effects of coupling between quasiparticles in the LLs and an E_{2g} phonon (200 meV) in graphene were calculated in theory and the phonon peaks of the E_{2g} phonon were predicted [40,41]. In their calculations, the relative intensity of the E_{2g} phonon peaks is predicted to be much weaker than that of the LLs [40,41]. Previous STS measurement also exhibits a slight signature of such phonon peaks [42]. However, our experiment shows that this is not the case for the K and K' out-of-plane phonons: the intensity of the phonon peaks is about 50 times than that of the LLs in the spectra (Fig. 1). The great enhancement of the K and K' out-of-plane phonon peaks can be attributed to the band mixing of the electrons at K and K' with the nearly free-electron states at Γ, which can effectively slow the decay of the K and K' out-of-plane phonons on the electronic wave functions in the vacuum [39].

To further understand the observed phonon peaks, we calculate electron-phonon self-energy considering the coupling of quasiparticles in LLs to the K and K' out-of-plane phonon with energy of 65 meV [40]. Here we concentrate only on the energy distributions of the phonon peaks on the DOS and ignore the contributions of LLs due to the quite weak signals obtained in our experiments. Figure 2(c) shows the obtained phonon peaks as a function of magnetic fields. Two peaks P_{0+} and P_{0-}, which are generated from the coupling of the LL_0 and the K and K' out-of-plane phonon, are independent of magnetic field. The other phonon peaks P_N (with $N \neq 0$) are generated from the LL_N, depending on the square root of both level index N and magnetic field B (SM Table S1 [35]). Obviously, the energies of the phonon peaks observed in our experiment [Fig. 1(d)] are reproduced quite well by our simulation. The only experimental feature that cannot be reproduced in our simulation is that all the phonon peaks split into two peaks with an energy separation of about 8 meV, which is invariable in different magnetic fields (see Figs. 1(c), 1(d), and SM Fig. S5 [35]). By considering the fine structure in the neighborhood of the phonon-emission threshold, these splittings are most likely corresponding to the bound states of an electron and a phonon via electron-phonon

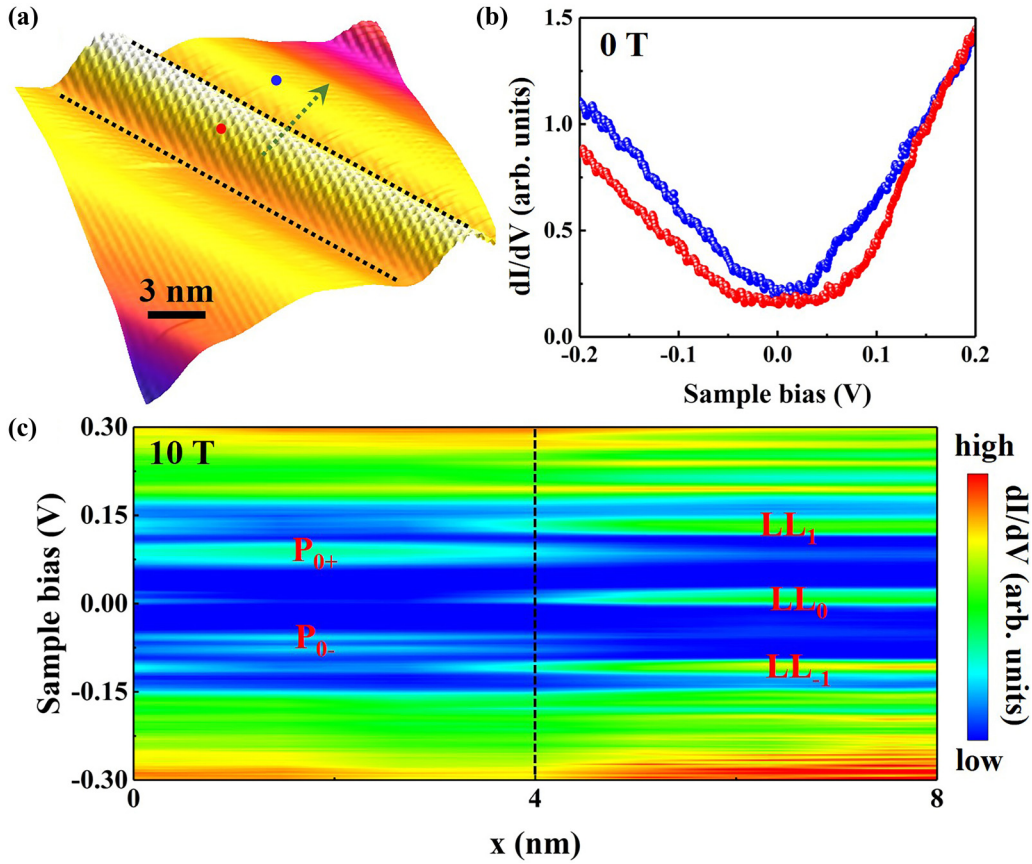

FIG. 3. Spatial variation of the dI/dV spectra around a graphene wrinkle. (a) A $20 \times 20\,\mathrm{nm}^2$ STM image of the typical graphene wrinkle in three-dimensional view ($V_b = 0.3\,\mathrm{mV}$, $I = 0.1\,\mathrm{nA}$). The dashed lines indicate the edges of the wrinkle. (b) Typical dI/dV spectra at $B = 0\,\mathrm{T}$ recorded at different positions in panel (a). The red and blue dots indicate the positions where we acquired the corresponding dI/dV spectra. (c) The evolution of the dI/dV spectra acquired at different spatial points along the green arrow of panel (a) in the magnetic field of $B = 10\,\mathrm{T}$. P_N and LL_N label the phonon peaks and LL peaks, respectively.

coupling [43]. Theoretically, the energy separation of the splitting in a phonon peak induced by the bound states can be estimated as $\alpha\omega_{ph}$, where α, the electron-phonon coupling parameter, is estimated to range from 0.04 to 0.13 in graphene [43]. In our experiment, $\alpha \sim 0.12$ is deduced according to the observed splitting.

III. MANIPULATION OF THE PHONON PEAKS

Previously, it has been demonstrated explicitly that the phonon-mediated tunneling spectra of graphene can be controlled by interaction between graphene and substrates [24–29,44–46]. In our sample, the interaction between graphene and the supporting substrate varies spatially due to the existence of nanoscale ripples or wrinkles. Figure 3(a) shows a representative STM image of graphene monolayer with a one-dimensional wrinkle. The tunneling spectrum acquired on the wrinkle exhibits a 130-meV gaplike feature pinned to the Fermi energy [red dots in Fig. 3(b)], implying the existence of the K and K' out-of-plane phonon excitations. However, the dI/dV spectrum acquired on the flat graphene region exhibits the V shape [blue dots in Fig. 3(b)], which directly reflects local DOS of massless Dirac fermions in graphene. Similar observations are obtained around many different graphene wrinkles with different STM tips. Such a result indicates that the interaction between graphene and substrates can sufficiently suppress the K and K' out-of-plane phonons of graphene and, consequently, weaken the inelastic tunneling channels. Our experiment in high magnetic fields, as shown subsequently, further demonstrates the possibilities to turn on/off the phonon peaks in the tunneling spectra. The local strain of the wrinkle can effectively enhance the strength of electron-phonon coupling [19,20], which may play an important role in switching the phonon peaks at nanoscale. Figure 3(c) shows the spatial-resolved dI/dV spectra recorded across the graphene wrinkle [the dotted arrow in Fig. 3(a)] by applying a magnetic field of 10 T (dI/dV spectra measured in different magnetic fields are shown in SM Figs. S6 and S7 [35]). High-quality well-defined LLs of the massless Dirac fermions in graphene monolayer are obtained off the wrinkle, as shown in the right part of Fig. 3(c), indicating that the dI/dV spectra on the flat region mainly reflect the local DOS of graphene. With approaching the top of the graphene wrinkle, two pronounced peaks (P_{0+} and P_{0-}), which are symmetric about the Dirac point (LL_0), appear and gradually increase in intensity. Simultaneously, the intensities of the LL_0 and $LL_{\pm1}$ decrease with approaching the wrinkle. On top of the graphene wrinkle, the signal of the phonon peaks is much stronger than that of the LLs in the spectra. Such a result is further verified by the atomic-scale dI/dV maps measured around the wrinkle

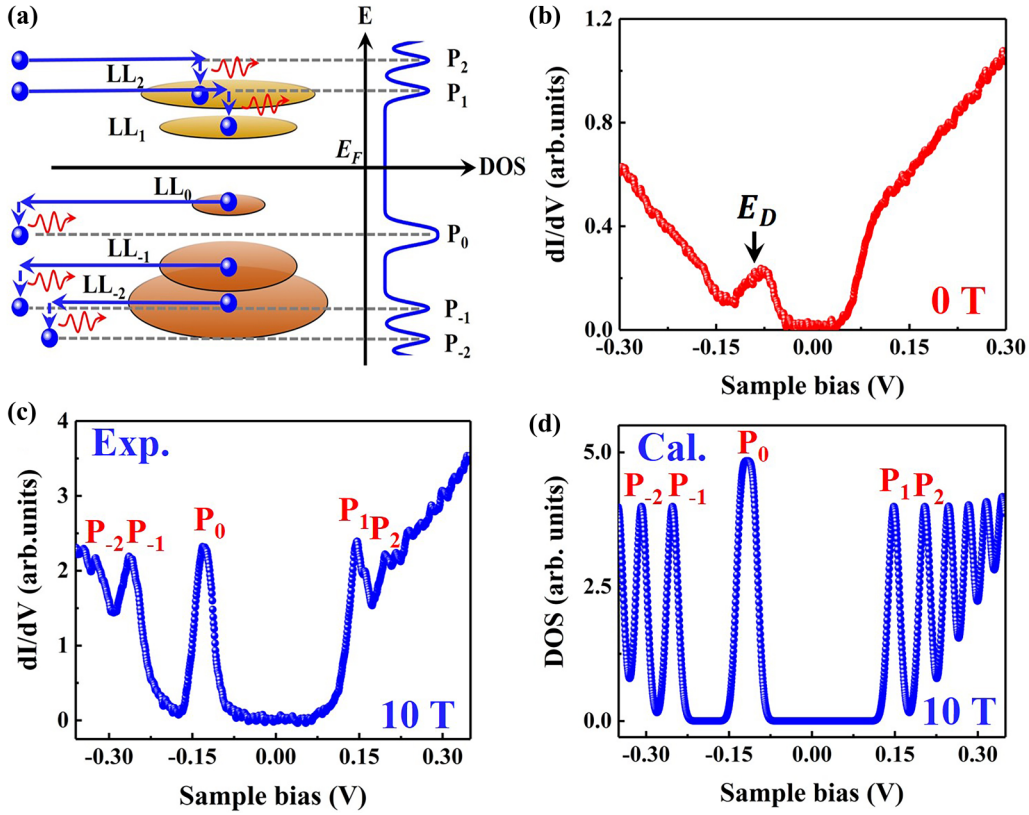

FIG. 4. The dI/dV spectra recorded on the graphene wrinkle with a large charge transfer. (a) Schematic of inelastic electron tunneling due to excitation of phonons with energy $\hbar\omega_{ph}$ at $B > 0$ T in a hole-doped region. The intrinsic LLs of graphene are shown as the numbered disks. (b) A typical dI/dV spectrum recorded on the graphene wrinkle at $B = 0$ T. The Dirac point, which is determined according to the zero LL in high magnetic field, is marked by the black arrow. (c) A typical dI/dV spectrum acquired on the graphene wrinkle at $B = 10$ T. P_N labels the phonon peaks. (d) Calculations of the DOS at $B = 10$ T by considering the coupling of the electron LLs and K and K' out-of-plane phonons in graphene.

(SM Fig. S8 [35]). Therefore, our experiment demonstrates explicitly the on/off of the phonon peaks at nanoscale.

Theoretically, the phonon peaks can be tuned by changing doping of graphene [40,41]. As schematically shown in Fig. 4(a), when the LL_0 is fully occupied, the LL_0 associated phonon mode appears only on one side of the Fermi level due to the Pauli exclusion principle (SM Table S1 [35]). In order to verify this doping-dependent phenomenon, we carry out similar high-field measurements in a graphene region that is electron doped. Figure 4(b) shows a representative zero-field STS spectrum of the studied graphene region, with the Dirac point well below the Fermi level due to the charge transfer between the topmost graphene layer and substrate. The Dirac point of the graphene monolayer is measured at about -70 meV according to the LL_0 measured in high magnetic field (SM Fig. S9 [35]). Figure 4(c) shows a typical dI/dV spectrum recorded in this region in a magnetic field of 10 T, and only one phonon peak associated to the LL_0 is observed, as marked by P_0. Our simulation of the energy distributions of the phonon peaks by taking into account the position of the LL_0, as shown in Fig. 4(d), reproduces well the experimental result.

Our experiment further demonstrates that it is possible to tune the phonon peaks by taking advantage of the STM tip pulse. By using a voltage pulse of 3 V for 0.1-s duration generated between the STM tip and the sample, we can locally enhance the van der Waals interactions between the topmost graphene sheet and the supporting substrate. Therefore, the K and K' out-of-plane phonon-mediated inelastic channel is suppressed and the phonon peaks become dramatically weak (SM Fig. S10 [35]). Moreover, our experiment demonstrates that the Fermi velocity in the graphene monolayer increases about 10% when the K and K' out-of-plane phonon is suppressed. Such a result agrees with the theoretical calculations that the electron-phonon interaction can reduce the Fermi velocity of the massless Dirac fermions to $v_F^{ep} = \frac{v_F^0}{1+\alpha}$, where v_F^0 is the Fermi velocity when the electron-phonon interaction is negligible [47,48]. According to the measured Fermi velocities, α is estimated as about 0.10, and consistent with that, ~ 0.12 as deduced from the electron-phonon bound states.

IV. CONCLUSION

In summary, we systematically study the electron-phonon coupling in a graphene monolayer and observe phonon peaks of the K and K' out-of-plane phonons in the tunneling spectra under high magnetic fields. Our experiments also show the ability to tune the phonon peaks at nanoscale by changing interactions between the graphene and substrate. The weak van der Waals interactions between graphene and the substrate can be used as an effective "switch" to turn the phonon peaks in graphene on or off.

ACKNOWLEDGMENTS

This work was supported by the National Natural Science Foundation of China (Grants No. 11974050 and No. 11674029). L.H. also acknowledges support from the National Program for Support of the Top-Notch Young Professionals, support from the Fundamental Research Funds for the Central Universities, and support from the Chang Jiang Scholars Program.

[1] F. Giustino, Electron-phonon interactions from first principles, Rev. Mod. Phys. **89**, 015003 (2017).

[2] J. Bardeen, L. N. Cooper, and J. R. Schrieffer, Microscopic theory of superconductivity, Phys. Rev. **106**, 162 (1957).

[3] J. Bardeen, L. N. Cooper, and J. R. Schrieffer, Theory of superconductivity, Phys. Rev. **108**, 1175 (1957).

[4] D. N. Basov, M. M. Fogler, A. Lanzara, F. Wang, and Y. Zhang, Colloquium: Graphene spectroscopy, Rev. Mod. Phys. **86**, 959 (2014).

[5] A. Bostwick, T. Ohta, T. Seyller, K. Horn, and E. Rotenberg, Quasiparticle dynamics in graphene, Nat. Phys. **3**, 36 (2007).

[6] A. C. Ferrari, J. C. Meyer, V. Scardaci, C. Casiraghi, M. Lazzeri, F. Mauri, S. Piscanec, D. Jiang, K. S. Novoselov, S. Roth, and A. K. Geim, Raman Spectrum of Graphene and Graphene Layers, Phys. Rev. Lett. **97**, 187401 (2006).

[7] J. Yan, Y. Zhang, P. Kim, and A. Pinczuk, Electric Field Effect Tuning of Electron-Phonon Coupling in Graphene, Phys. Rev. Lett. **98**, 166802 (2007).

[8] E. J. Nicol and J. P. Carbotte, Phonon spectroscopy through the electronic density of states in graphene, Phys. Rev. B **80**, 081415(R) (2009).

[9] J. P. Carbotte, E. J. Nicol, and S. G. Sharapov, Effect of electron-phonon interaction on spectroscopies in graphene, Phys. Rev. B **81**, 045419 (2010).

[10] A. Pound, J. P. Carbotte, and E. J. Nicol, Magneto-optical conductivity in graphene including electron-phonon coupling, Phys. Rev. B **85**, 125422 (2012).

[11] M. O. Goerbig, Electronic properties of graphene in a strong magnetic field, Rev. Mod. Phys. **83**, 1193 (2011).

[12] C. Faugeras, M. Amado, P. Kossacki, M. Orlita, M. Sprinkle, C. Berger, W. A. de Heer, and M. Potemski, Tuning the Electron-Phonon Coupling in Multilayer Graphene with Magnetic Fields, Phys. Rev. Lett. **103**, 186803 (2009).

[13] J. Yan, S. Goler, T. D. Rhone, M. Han, R. He, P. Kim, V. Pellegrini, and A. Pinczuk, Observation of Magnetophonon Resonance of Dirac Fermions in Graphite, Phys. Rev. Lett. **105**, 227401 (2010).

[14] P. Kossacki, C. Faugeras, M. Kuhne, M. Orlita, A. A. L. Nicolet, J. M. Schneider, D. M. Basko, Y. I. Latyshev, and M. Potemski, Electronic excitations and electron-phonon coupling in bulk graphite through Raman scattering in high magnetic fields, Phys. Rev. B **84**, 235138 (2011).

[15] Y. Kim, Y. Ma, A. Imambekov, N. G. Kalugin, A. Lombardo, A. C. Ferrari, J. Kono, and D. Smirnov, Magnetophonon resonance in graphite: High-field Raman measurements and electron-phonon coupling contributions, Phys. Rev. B **85**, 121403(R) (2012).

[16] S. Rémi, B. B. Goldberg, and A. K. Swan, Charge Tuning of Nonresonant Magnetoexciton Phonon Interactions in Graphene, Phys. Rev. Lett. **112**, 056803 (2014).

[17] P. Leszczynski, Z. Han, A. A. L. Nicolet, B. A. Piot, P. Kossacki, M. Orlita, V. Bouchiat, D. M. Basko, M. Potemski, and C. Faugeras, Electrical switch to the resonant magneto-phonon effect in graphene, Nano Lett. **14**, 1460 (2014).

[18] A. H. Castro Neto and F. Guinea, Electron-phonon coupling and Raman spectroscopy in graphene, Phys. Rev. B **75**, 045404 (2007).

[19] C. Si, Z. Liu, W. Duan, and F. Liu, First-Principles Calculations on the Effect of Doping and Biaxial Tensile Strain on Electron-Phonon Coupling in Graphene, Phys. Rev. Lett. **111**, 196802 (2013).

[20] C. Si, Z. Suna, and F. Liu, Strain engineering of graphene: A review, Nanoscale, **8**, 3207 (2016).

[21] Y. Zhang, V. W. Brar, F. Wang, C. Girit, Y. Yayon, M. Panlasigui, A. Zettl, and M. F. Crommie, Giant phonon-induced conductance in scanning tunnelling spectroscopy of gate-tunable graphene, Nat. Phys. **4**, 627 (2008).

[22] V. W. Brar, S. Wickenburg, M. Panlasigui, C. Park, T. O. Wehling, Y. Zhang, R. Decker, C. Girit, A. V. Balatsky, S. G. Louie, A. Zettl, and M. F. Crommie, Observation of Carrier-Density-Dependent Many-Body Effects in Graphene via Tunneling Spectroscopy, Phys. Rev. Lett. **104**, 036805 (2010).

[23] F. D. Natterer, Y. Zhao, J. Wyrick, Y. Chan, W. Ruan, M. Chou, K. Watanabe, T. Taniguchi, N. B. Zhitenev, and J. A. Stroscio, Strong Asymmetric Charge Carrier Dependence in Inelastic Electron Tunneling Spectroscopy of Graphene Phonons, Phys. Rev. Lett. **114**, 245502 (2015).

[24] H. W. Kim, W. Ko, J. Ku, I. Jeon, D. Kim, H. Kwon, Y. Oh, S. Ryu, Y. Kuk, S. W. Hwang, and H. Suh, Nanoscale control of phonon excitations in graphene, Nat. Commun. **6**, 7528 (2015).

[25] J. Červenka, K. van de Ruit, and C. F. J. Flipse, Giant inelastic tunneling in epitaxial graphene mediated by localized states, Phys. Rev. B **81**, 205403 (2010).

[26] U. Chandni, K. Watanabe, T. Taniguchi, and J. P. Eisenstein, Signatures of phonon and defect-assisted tunneling in planar metal−hexagonal boron nitride−graphene junctions, Nano Lett. **16**, 7982 (2016).

[27] N. Néel, C. Steinke, T. O. Wehling, and J. Kröger, Inelastic electron tunneling into graphene nanostructures on a metal surface, Phys. Rev. B **95**, 161410(R) (2017).

[28] E. Minamitani, R. Arafune, T. Frederiksen, T. Suzuki, S. M. F. Shahed, T. Kobayashi, N. Endo, H. Fukidome, S. Watanabe, and T. Komeda, Atomic-scale characterization of the interfacial phonon in graphene/SiC, Phys. Rev. B **96**, 155431 (2017).

[29] S. Li, K. Bai, W. Zuo, Y. Liu, Z. Fu, W. Wang, Y. Zhang, L. Yin, J. Qiao, and L. He, Tunneling Spectra of a Quasifreestanding Graphene Monolayer, Phys. Rev. Appl. **9**, 054031 (2018).

[30] S. Tanaka, M. Matsunami, and S. Kimura, An investigation of electron-phonon coupling via phonon dispersion measurements in graphite using angle-resolved photoelectron spectroscopy, Sci. Rep. **3**, 3031 (2013).

[31] Y. Liu, L. Zhang, M. K. Brinkley, G. Bian, T. Miller, and T. C. Chiang, Phonon-Induced Gaps in Graphene and Graphite Observed by Angle-Resolved Photoemission, Phys. Rev. Lett. **105**, 136804 (2010).

[32] P. Ayria, S. Tanaka, A. R. T. Nugraha, M. S. Dresselhaus, and R. Saito, Phonon-assisted indirect transitions in angle-resolved photoemission spectra of graphite and graphene, Phys. Rev. B **94**, 075429 (2016).

[33] K. Bai, Y. Zhou, H. Zheng, L. Meng, H. Peng, Z. Liu, J. Nie, and L. He, Creating One-Dimensional Nanoscale Periodic Ripples in a Continuous Mosaic Graphene Monolayer, Phys. Rev. Lett. **113**, 086102 (2014).

[34] D. Ma, Z. Fu, X. Sui, K. Bai, J. Qiao, C. Yan, Y. Zhang, J. Hu, Q. Xiao, X. Mao, W. Duan, and L. He, Modulating the electronic properties of graphene by self-organized sulfur identical nanoclusters and atomic superlattices confined at an interface, ACS Nano **12**, 10984 (2018).

[35] See Supplemental Material at http://link.aps.org/supplemental/10.1103/PhysRevB.100.075435 for more experimental data, analysis, and discussion.

[36] M. Mohr, J. Maultzsch, E. Dobardžić, S. Reich, I. Milošević, M. Damnjanović, A. Bosak, M. Krisch, and C. Thomsen, Phonon dispersion of graphite by inelastic x-ray scattering, Phys. Rev. B **76**, 035439 (2007).

[37] D. L. Miller, K. D. Kubista, G. M. Rutter, M. Ruan, W. A. de Heer, P. N. First, and J. A. Stroscio, Observing the quantization of zero mass carriers in graphene, Science **324**, 924 (2009).

[38] L. Yin, S. Li, J. Qiao, J. Nie, and L. He, Landau quantization in graphene monolayer, Bernal bilayer, and Bernal trilayer on graphite surface, Phys. Rev. B **91**, 115405 (2015).

[39] T. O. Wehling, I. Grigorenko, A. I. Lichtenstein, and A. V. Balatsky, Phonon-Mediated Tunneling into Graphene, Phys. Rev. Lett. **101**, 216803 (2008).

[40] A. Pound, J. P. Carbotte, and E. J. Nicol, Effects of electron-phonon coupling on Landau levels in graphene, Phys. Rev. B **84**, 085125 (2011).

[41] A. Pound, J. P. Carbotte, and E. J. Nicol, Phonon structures in the electronic density of states of graphene in magnetic field, EPL **94**, 57006 (2011).

[42] Y. J. Song, A. F. Otte, Y. Kuk, Y. Hu, D. B. Torrance, P. N. First, W. A. de Heer, H. Min, S. Adam, M. D. Stiles, A. H. MacDonald, and J. A. Stroscio, High-resolution tunnelling spectroscopy of a graphene quartet, Nature (London) **467**, 185 (2010).

[43] J. Zhu, S. M. Badalyan, and F. M. Peeters, Electron-Phonon Bound States in Graphene in a Perpendicular Magnetic Field, Phys. Rev. Lett. **109**, 256602 (2012).

[44] S. Jung, M. Park, J. Park, T. Jeong, H. Kim, K. Watanabe, T. Taniguchi, D. H. Ha, C. Hwang, and Y. Kim, Vibrational properties of h-BN and h-BN-graphene heterostructures probed by inelastic electron tunneling spectroscopy, Sci. Rep. **5**, 16642 (2015).

[45] E. E. Vdovin, A. Mishchenko, M. T. Greenaway, M. J. Zhu, D. Ghazaryan, A. Misra, Y. Cao, S. V. Morozov, O. Makarovsky, T. M. Fromhold, A. Patanè, G. J. Slotman, M. I. Katsnelson, A. K. Geim, K. S. Novoselov, and L. Eaves, Phonon-Assisted Resonant Tunneling of Electrons in Graphene–Boron Nitride Transistors, Phys. Rev. Lett. **116**, 186603 (2016).

[46] J. Halle, N. Neel, M. Fonin, M. Brandbyge, and J. Kröger, Understanding and engineering phonon-mediated tunneling into graphene on metal surfaces, Nano. Lett. **18**, 5697 (2018).

[47] C. Park, F. Giustino, M. L. Cohen, and S. G. Louie, Velocity Renormalization and Carrier Lifetime in Graphene from the Electron-Phonon Interaction, Phys. Rev. Lett. **99**, 086804 (2007).

[48] W. Tse and S. D. Sarma, Phonon-Induced Many-Body Renormalization of the Electronic Properties of Graphene, Phys. Rev. Lett. **99**, 236802 (2007).